

A Hybrid Multiport Modular Multilevel DC-DC Converter For Offshore Wind Farms Application

Fei Zhang, Géza Joós

Department of Electrical and Computer Engineering
 McGill University
 Montréal, Canada
 fei.zhang@mail.mcgill.ca

Wei Li, Weihua Wang

OPAL-RT Technologies
 Montréal, Canada
 wei.li@opal-rt.com

Abstract—Offshore wind farms connected with HVDC transmission line is a promising solution to bring the power to shore and assure the system efficiency. A DC-DC converter with high step ratio is required for such application. The modular multilevel converter (MMC) for transformer-less DC-DC converter application is regarded as an alternative solution to replace the two-stage DC-AC-DC conversion. A hybrid multiport modular multilevel DC-DC converter is proposed in this paper, which have one high voltage port and multiple low voltage ports. The low voltage ports can be connected to the dc output of wind turbines. The bidirectional power flow is realized by controlling the arm voltages. The proposed converter has a lower circulating currents as compared to the single-port MMC DC-DC converter. By using the full bridge submodules (FBSMs), the converter also has DC fault blocking capability.

Index Terms—modular multilevel converter, DC-DC converter.

I. INTRODUCTION

With the increasing number of high voltage DC (HVDC) transmission lines being installed all over the world, the research on DC grid is becoming more and more interesting for industry and academia [1]-[5]. With a high penetration of renewable energies, medium voltage DC (MVDC) distribution grid is considered as more efficient than AC distribution grid [6]-[8]. In order to reduce the loss, offshore wind farms located far away from the shore require HVDC lines to transfer the power. High power DC-DC converter is needed to boost the low voltage output of wind generators to connect to the MVDC collection point [9].

Benefited by the advantages of high efficiency, good harmonic performance and modularity, modular multilevel converter (MMC) has been widely used in high power applications. The application of MMC for DC-AC conversion including HVDC, FACTS and motor drive has been presented in [10]-[15]. The MMC for DC-DC conversion is also attracting more attention. The conventional MMC topology for DC-DC conversion is the front to front connection of two MMCs, which has two cascaded DC-AC stages. An intermediate transformer is required [16]-[20], which results in an increased size and cost of the system. Although medium

frequency transformer can be adopted to reduce the size, soft switching is required to reduce the loss caused by the increased switching frequency. However, soft switching of MMC is difficult to implement.

The MMC for transformer-less DC-DC conversion has been investigated in [21]-[23]. Different from the MMC for DC-AC application where the AC current flows through the upper and lower arm to the AC grid, the transformer-less MMC DC-DC converter has the AC current circulating inside the phases to balance the power between the upper and lower arms. A large inductor filter is needed to block the AC components from appearing at the low voltage DC side, as shown in Fig. 1. The AC circulating current will become large if the voltage conversion ratio increases, which results in a high loss and a high current rating of the switches. Thus, the single-port transformer-less MMC DC-DC converter is ideal for connecting two DC links with a small voltage step ratio close to 2:1 [24].

In this paper, a hybrid modular multilevel DC-DC converter topology with multiple ports is proposed. The upper arm adopts the half bridge submodules (HBSMs), and the SMs of lower arm are connected to the low voltage output of wind generators. Full bridge submodules (FBSMs) are used to block the DC fault happens on the high voltage side. The proposed topology has a high voltage conversion ratio while the circulating current is

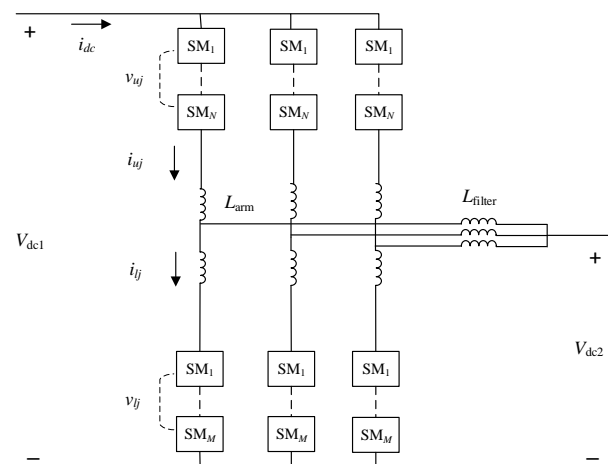


Fig. 1. Single-port transformer-less MMC DC-DC converter.

kept small by flexibly choosing the AC component of the upper and lower arm voltages. The system has a high reliability. It can operate by adjusting the AC voltages if some of the low voltage DC links are disconnected, which does not require the overdesigned of the system. The bidirectional power flow is realized by controlling the arm voltages.

II. PROPOSED HYBRID MULTIPORT DC-DC CONVERTER

A. Proposed Topology

The proposed three-phase topology is shown in Fig. 2. Based on the differences of the components, the SMs are divided into two groups, including HBSMs and FBSMs. The upper arm is composed by standard HBSMs, while the lower arm is composed by FBSMs. The FBSMs have extra ports that can connect to the low voltage wind generators. The equivalent circuit of the three-phase system is shown in Fig. 3. The upper arm voltage contains DC and AC components, while the lower arm voltage only contains AC component. The blue line represents the DC current flow loop and the red line represents the AC current flow loop.

B. Steady-State Analysis

According to the equivalent circuit in Fig. 3. The upper arm and lower arm voltages are defined as

$$v_{upi} = v_{upi_AC} + v_{upi_DC} \quad (1)$$

$$v_{lowi} = v_{lowi_AC} \quad (2)$$

where, i represents the phase, v_{upi_AC} and v_{upi_DC} represents the AC component and DC component of upper arm, respectively. v_{lowi_AC} represents the AC component of lower arm.

From KVL, the relationship between the voltages can be expressed as

$$V_{MVDC} = v_{upi_AC} + v_{upi_DC} + v_{lowi_AC} + L_{arm} \frac{di_{ciri}}{dt} \quad (3)$$

where, V_{MVDC} represents the medium voltage DC, and i_{ciri} represents the AC current which circulate between the arms.

The system can be further decoupled into DC and AC loops, which is derived as

$$V_{MVDC} = v_{upi_DC} \quad (4)$$

$$v_{upi_AC} + v_{lowi_AC} + L_{arm} \frac{di_{ciri}}{dt} = 0 \quad (5)$$

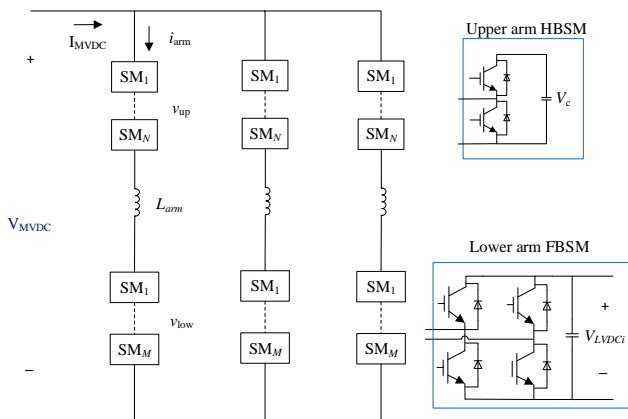


Fig. 2. Proposed three-phase multiport MMC DC-DC converter.

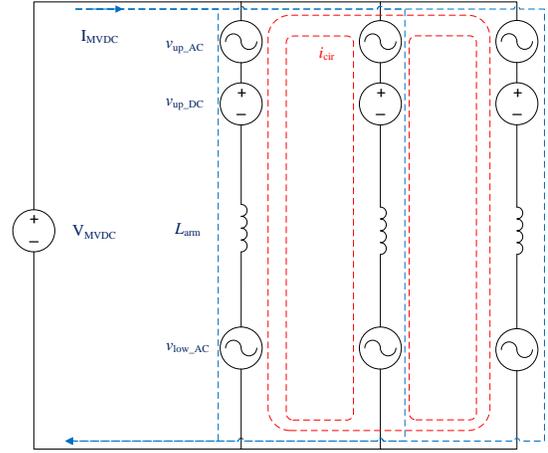


Fig. 3. Equivalent circuit of three-phase multiport MMC DC-DC

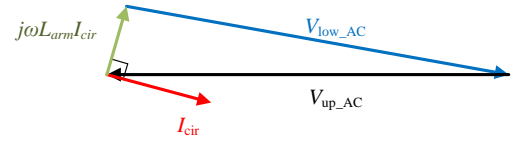


Fig. 4. Phasor diagram of the AC loop.

According to (5), the phasor diagram of the AC loop is shown in Fig. 4.

The arm current is expressed as

$$i_{armi} = \frac{1}{3} i_{MVDC} + i_{ciri} \quad (6)$$

In steady-state, the energy in the upper arm should be kept constant, which means the DC component of the upper arm power should be zero, otherwise the upper arm energy will keep increasing or decreasing. If only the fundamental frequency is considered, the AC components of arm voltages can be expressed as

$$v_{upi_AC} = V_{upi_AC} \cos(\omega t) \quad (7)$$

$$v_{lowi_AC} = V_{lowi_AC} \cos(\omega t + \theta) \quad (8)$$

where, ω is the angular frequency, and θ is the phase shift between the upper and lower arm which controls the power flow direction.

From (5), (7) and (8), the AC current i_{ciri} is calculated as

$$i_{ciri} = -\frac{1}{\omega L_{arm}} (V_{upi_AC} \sin(\omega t) + V_{lowi_AC} \sin(\omega t + \theta)) \quad (9)$$

Then, the power of upper and lower arm is calculated as

$$P_{upi} = v_{upi} i_{upi} = (v_{upi_AC} + v_{upi_DC}) \cdot \left(\frac{1}{3} i_{MVDC} + i_{ciri} \right) \quad (10)$$

$$P_{lowi} = v_{lowi} i_{lowi} = v_{lowi_AC} \cdot \left(\frac{1}{3} i_{MVDC} + i_{ciri} \right) \quad (11)$$

From (10) and (11), the DC parts of the upper and lower arm power are calculated as

$$P_{upi_DC} = -\frac{1}{2\omega L_{arm}} V_{upi_AC} V_{lowi_AC} \sin(\theta) + \frac{1}{3} V_{MVDC} i_{MVDC} \quad (12)$$

$$P_{lowi_DC} = \frac{1}{2\omega L_{arm}} V_{upi_AC} V_{lowi_AC} \sin(\theta) \quad (13)$$

If the input power is equal to the output power, the DC

component of upper arm power is zero in (12). The equation of the transferred power of the system is derived as

$$P = V_{MVDC} i_{MVDC} = \frac{3V_{upi_AC} V_{lowi_AC} \sin(\theta)}{2\omega L_{arm}} \quad (14)$$

From (14), the bidirectional power flow can be realized by control the angle θ . V_{upi_AC} and V_{lowi_AC} should be maximized to get the high power transfer capability and make the full utilization of the switches. In the single-port MMC DC-DC topology, there will be a high circulating current if the difference between the upper arm voltage and lower arm voltage is large. Thus, the single-port MMC DC-DC topology is optimal for low voltage step ratio application. In the proposed topology, by stacking the low voltage DC ports, V_{upi_AC} and V_{lowi_AC} can be designed with close value.

III. PREDICTIVE CURRENT CONTROL AND SORTING STRATEGY

The predictive current control is adopted in this paper to control the AC current which circulates inside the converter. The control diagram is shown in Fig. 5. For the upper arm, the reference voltage is fixed which is defined as

$$v_{upi_AC}^{ref} = ma \cdot v_{upi_DC} \cos(\omega t) \quad (15)$$

Based on (5), the forward euler method is used to derive the discrete-time model of the system

$$v_{upi_AC}(k) + v_{lowi_AC}(k) + L_{arm} \frac{i_{ciri}(k+1) - i_{ciri}(k)}{T_s} = 0 \quad (16)$$

where, $v_{upi_AC}(k)$ and $i_{ciri}(k)$ is the measured value at time k . $i_{ciri}(k+1)$ is the circulating current at time $k+1$.

The reference voltage of the lower arm is calculated by the predictive current control. In (16), $i_{ciri}(k+1)$ is replaced by its reference value, then

$$v_{lowi_AC}^{ref}(k) = -v_{upi_AC}(k) - L_{arm} \frac{i_{ciri}^{ref}(k+1) - i_{ciri}(k)}{T_s} \quad (17)$$

The references of arm voltages are calculated as

$$v_{upi} = v_{upi_AC}^{ref} + V_{MVDC} \quad (18)$$

$$v_{lowi} = v_{lowi_AC}^{ref} \quad (19)$$

The AC current reference is obtained by the power and upper arm AC voltage reference. The reference of active power is obtained by the balancing control of the sum of the capacitor voltages in each valve. The individual capacitor voltages are balanced by the sorting strategy, which has a tolerance band as shown in Fig. 6. Δn is the required modification on-state SMs at current step. The number of SMs that exceed tolerance band of

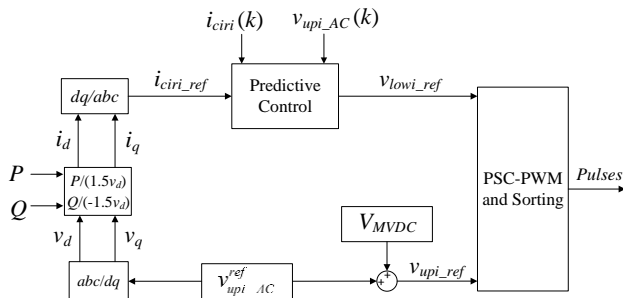


Fig. 5. Diagram of the control strategy.

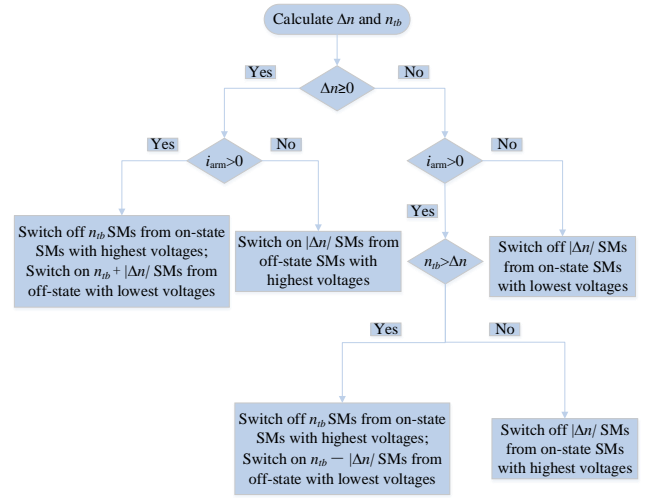


Fig. 6. Flowchart of sorting strategy.

the nominal capacitor voltage is denoted as n_{tb} . This sorting strategy is applied for the HBSMs.

IV. PERFORMANCE RESULTS

The real-time MMC model developed by OPAL-RT is used to validate the proposed topology and control strategy. The performance is tested by steady-state and transient-state operation. The power is transferred from the low voltage side to the high voltage side. The system parameters are shown in Table I.

A. Steady-state Performance

In this scenario, the converter is connecting multiple low voltage DC sources with 1 kV to a 20 kV DC load. The power rating is 20 MW. The results are shown in Fig. 7. In Fig. 7 (a), the MVDC voltage is kept close to 20 kV. The DC current in Fig. 7 (b) is negative since the power is transferred from low voltage side to high voltage side. The arm current is shown in Fig. 7 (c) which has the DC component and AC component. The upper arm voltage is shown in Fig. 7 (d), which has a 20 kV DC component voltage. The lower arm voltage is shown in Fig. 7 (e), which is a pure AC voltage. The average capacitor

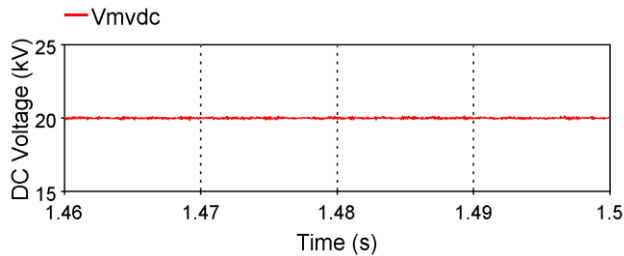
Table I. System parameters

Parameter	Symbol	Value
Power rating	P	20 MW
Sampling time step	T_s	25 us
Number of upper SMs	N	40
Number of lower SMs	M	20
MVDC voltage	V_{MVDC}	20 kV
LVDC voltage	V_{LVDC}	1 kV
AC frequency	f_{circ}	180 Hz
Carrier frequency	f	600 Hz
Arm inductance	L_{arm}	10 mH
SM capacitance	C	5 mF

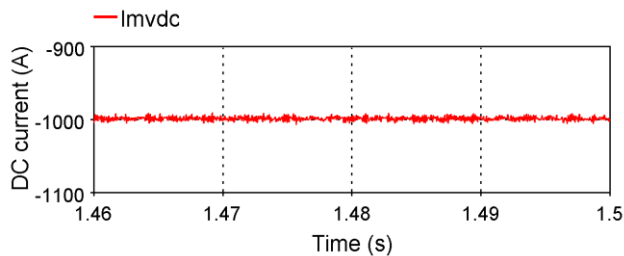
voltages are shown in Fig. 7 (f), and several individual capacitor voltages are shown in Fig. 7 (g). The capacitor voltages are maintained close to 1 kV the nominal capacitor voltage.

B. Transient-state Performance

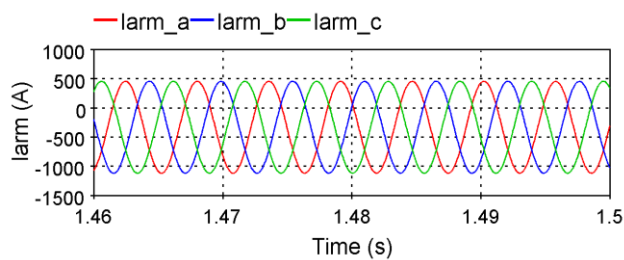
The transient-state results are shown in Fig. 8. A power step from 10 MW to 20 MW is enabled at $t=1s$. In order to investigate the transient-state performance, the value of resistor



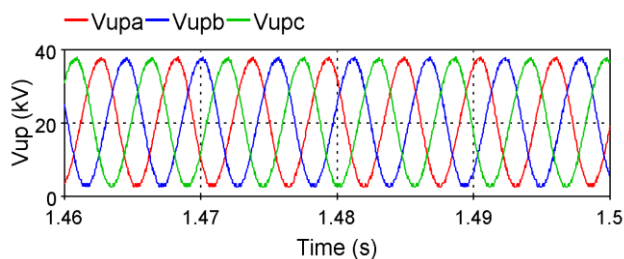
(a) MVDC voltage



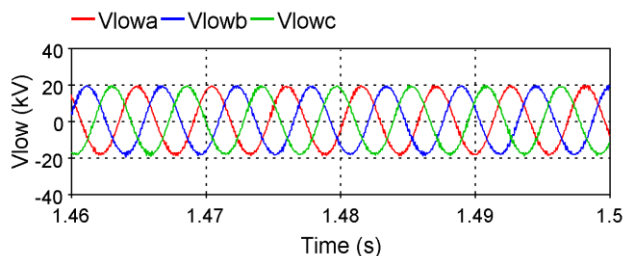
(b) MVDC current



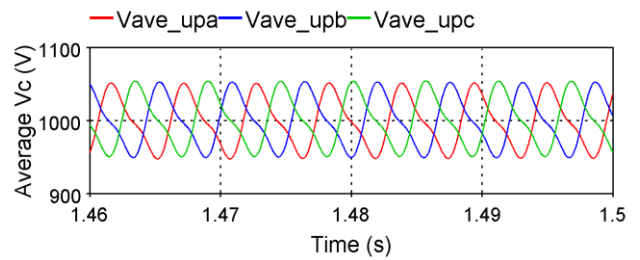
(c) Arm current



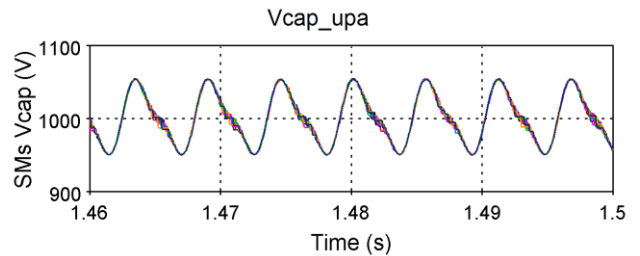
(d) Upper arm voltage



(e) Lower arm voltage



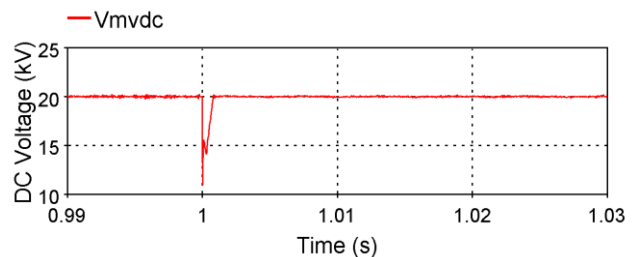
(f) Average capacitor voltage of upper arm



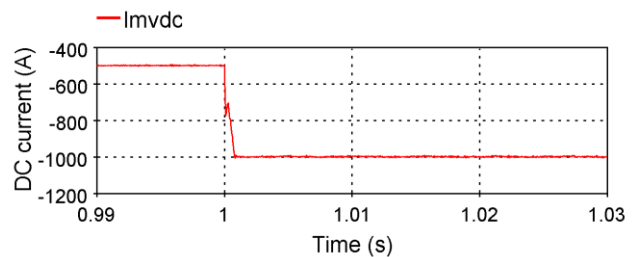
(g) Individual capacitor voltage of phase a

Fig. 7. Simulation results during steady-state.

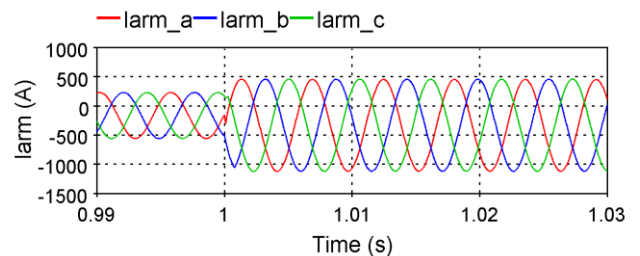
load at the high voltage side is reduced by half when the power step happens. From Fig. 8, the system reaches the steady-state very fast. The fast dynamic response of MVDC current and arm current are achieved by the predictive control, which are shown in Fig 8. (b) and (c). The capacitor voltages of SMs are also quickly balanced during the transient operation as shown in Fig.



(a) MVDC voltage



(b) MVDC current



(c) Arm current

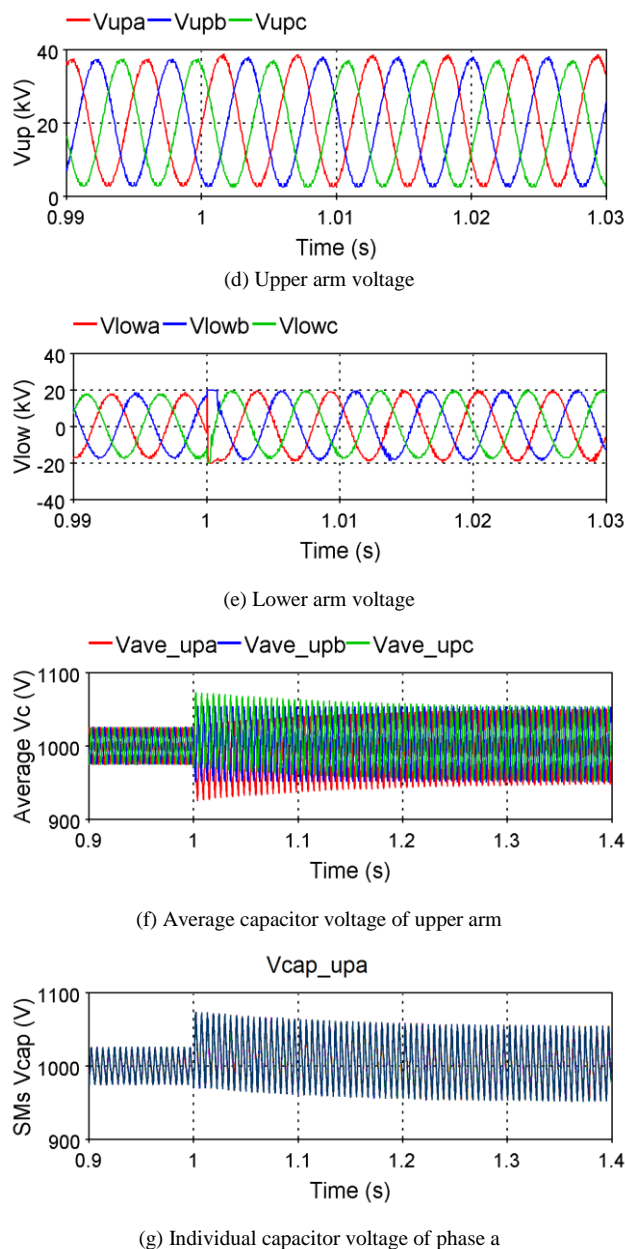


Fig. 8. Simulation results during transient-state.

8 (f) and (g).

V. CONCLUSION

In this paper, a hybrid transformer-less multiport modular multilevel DC-DC converter is proposed to connect offshore wind farms to a medium voltage DC collection point. The proposed topology has multiple DC interfaces which can connect to the wind generators. Compared to the single-port MMC DC-DC converter, a high voltage conversion ratio is achieved with a small circulating current. The converter has the capability of bidirectional power flow control by adjusting the phase difference between the arm voltages. The predictive control method is used to control the arm current. Both steady-state and transient-state performances of the proposed topology are validated by simulation.

REFERENCES

- [1] N. Flourentzou, V. G. Agelidis and G. D. Demetriades, "VSC-Based HVDC Power Transmission Systems: An Overview," *IEEE Transactions on Power Electronics*, vol. 24, no. 3, pp. 592-602, March 2009.
- [2] M. Saedifard and R. Iravani, "Dynamic Performance of a Modular Multilevel Back-to-Back HVDC System," *IEEE Transactions on Power Delivery*, vol. 25, no. 4, pp. 2903-2912, Oct. 2010.
- [3] H. Liu, K. Ma, Z. Qin, P. C. Loh and F. Blaabjerg, "Lifetime Estimation of MMC for Offshore Wind Power HVDC Application," *IEEE Journal of Emerging and Selected Topics in Power Electronics*, vol. 4, no. 2, pp. 504-511, June 2016.
- [4] G. Pinares and M. Bongiorno, "Modeling and Analysis of VSC-Based HVDC Systems for DC Network Stability Studies," *IEEE Transactions on Power Delivery*, vol. 31, no. 2, pp. 848-856, April 2016.
- [5] J. Lin, "Integrating the First HVDC-Based Offshore Wind Power into PJM System-A Real Project Case Study," *IEEE Transactions on Industry Applications*, vol. 52, no. 3, pp. 1970-1978, June 2016.
- [6] C. Meyer, M. Hoing, A. Peterson and R. W. De Doncker, "Control and Design of DC Grids for Offshore Wind Farms," *IEEE Transactions on Industry Applications*, vol. 43, no. 6, pp. 1475-1482, Nov. 2007.
- [7] F. Mura and R. W. De Doncker, "Design aspects of a medium-voltage direct current (MVDC) grid for a university campus," in *Proc. IEEE Eighth Int. Conf. Power Electron. ECCE Asia*, pp. 2359-2366, 2011.
- [8] H. A. B. Siddique, S. M. Ali, and R. W. De Doncker, "DC collector grid configurations for large photovoltaic parks," in *Proc. 15th Eur. Conf. Power Electron.*, pp. 1-10, April, 2013.
- [9] W. Chen, A. Q. Huang, C. Li, G. Wang and W. Gu, "Analysis and Comparison of Medium Voltage High Power DC/DC Converters for Offshore Wind Energy Systems," *IEEE Transactions on Power Electronics*, vol. 28, no. 4, pp. 2014-2023, April 2013.
- [10] A. Lesnicar and R. Marquardt, "An innovative modular multilevel converter topology suitable for a wide power range," in *Proc. IEEE Bologna Power Tech Conf.*, vol. 3, pp. 1-6, Jun. 2003.
- [11] M. Hagiwara, K. Nishimura, and H. Akagi, "A medium-voltage motor drive with a modular multilevel PWM inverter," *IEEE Transactions on Power Electronics*, vol. 25, no. 7, pp. 1786-1799, Jul. 2010.
- [12] S. Rohner, S. Bernet, M. Hiller, and R. Sommer, "Modulation, losses, and semiconductor requirements of modular multilevel converters," *IEEE Transactions on Industrial Electronics*, vol. 57, no. 8, pp. 2633-2642, Aug. 2010.
- [13] H. P. Mohammadi, and M. T. Bina, "A transformerless medium-voltage STATCOM topology based on extended modular multilevel converters," *IEEE Transactions on Power Electronics*, vol. 26, no. 5, pp. 1534-1545, May 2011.
- [14] L. Harnefors, A. Antonopoulos, S. Norrga, L. Angquist, and H.-P. Nee, "Dynamic analysis of modular multilevel converters," *IEEE Transactions on Industrial Electronics*, vol. 60, pp. 2526-2537, Jul. 2013.
- [15] A. Nami, J. Liang, F. Dijkhuizen, and G. Demetriades, "Modular multilevel converters for HVDC applications: Review on converter cells and functionalities," *IEEE Transactions on Power Electronics*, vol. 30, pp. 18-36, Jan. 2015.
- [16] C. D. Barker, C. C. Davidson, D. R. Trainer, and R. S. Whitehouse, "Requirements of DC-DC Converters to facilitate large DC grids," in *Proc. CIGRE Symp.*, Paris, France, pp. 1-10, Aug. 2012.
- [17] T. Luth, M. Merlin, T. Green, F. Hassan, and C. Barker, "High-frequency operation of a DC/AC/DC system for HVDC applications," *IEEE Transactions on Power Electronics*, vol. 29, pp. 4107-4115, Aug. 2014.
- [18] S. Kenzelmann, A. Rufer, D. Dujic, F. Canales, and Y. R. de Novaes, "Isolated DC/DC structure based on modular multilevel converter," *IEEE Transactions on Power Electronics*, vol. 30, no. 1, pp. 89-98, Jan. 2015.
- [19] S.P. Engel, M. Stieneker, N. Soltan, S. Rabiee, H. Stage and R.W. De Doncker, "Comparison of the modular multilevel DC converter and the dual-active bridge converter for power conversion in HVDC and MVDC grids," *IEEE Transactions on Power Electronics*, vol. 30, no. 1, pp. 124-137, Jan. 2015.
- [20] I. A. Gowaid, G. P. Adam, A. M. Massoud, S. Ahmed, D. Holliday, and B. W. Williams, "Quasi two-level operation of modular multilevel converter for use in a high-power DC transformer with DC fault isolation capability," *IEEE Transactions on Power Electronics*, vol. 30, no. 1, pp. 108-123, Jan. 2015.
- [21] S. Norrga, L. Angquist, and A. Antonopoulos, "The polyphase cascaded cell DC/DC converter," in *IEEE Energy Conversion Congress and Exposition*, pp. 4082-4088, Sept. 2013.

- [22] J. Ferreira, "The multilevel modular DC converter," *IEEE Transactions on Power Electronics*, vol. 28, pp. 4460–4465, Oct. 2013.
- [23] G. Kish, M. Ranjram, and P. Lehn, "A modular multilevel DC/DC converter with fault blocking capability for HVDC interconnects," *IEEE Transactions on Power Electronics*, vol. 30, pp. 148–162, Jan. 2015.
- [24] T. Luth, M. M. C. Merlin, and T. C. Green, "Modular multilevel DC/DC converter architectures for HVDC taps," in *Power Electronics and Applications (EPE'14-ECCE Europe)*, pp.1-10, Aug. 2014.